Ring Size of Somatostatin Analogues (ODT-8) Modulates Receptor Selectivity and Binding Affinity

Judit Erchegyi,[†] Christy Rani R. Grace,[‡] Manoj Samant,[†] Renzo Cescato,[§] Veronique Piccand,[§] Roland Riek,[‡] Jean Claude Reubi,[§] and Jean E. Rivier*,[†]

The Clayton Foundation Laboratories for Peptide Biology and Structural Biology Laboratory, The Salk Institute for Biological Studies, 10010 North Torrey Pines Road, La Jolla, California 92037, and Division of Cell Biology and Experimental Cancer Research, Institute of Pathology, University of Berne, Berne, Switzerland 3012

Received November 15, 2007

The synthesis, biological testing, and NMR studies of several analogues of H-c[Cys^3-Phe^6-Phe^7-DTrp^8-Lys^9-Thr^{10}-Phe^{11}-Cys^{14}]-OH (ODT-8, a pan-somatostatin analogue, **1**) have been performed to assess the effect of changing the stereochemistry and the number of atoms in the disulfide bridge on binding affinity. Cysteine at positions 3 and/or 14 (somatostatin numbering) were/was substituted with D-cysteine, norcysteine, D-norcysteine, homocysteine, and/or D-homocysteine. The 3D structure analysis of selected partially selective, bioactive analogues (**3**, **18**, **19**, and **21**) was carried out in dimethylsulfoxide. Interestingly and not unexpectedly, the 3D structures of these analogues comprised the pharmacophore for which the analogues had the highest binding affinities (i.e., sst$_4$ in all cases).

Introduction

Somatostatin (SRIF)[a] is a major endocrine hormone with multiple physiological actions[1–11] modulated by one or more of the five SRIF receptors.[12–16] The biological role, as well as the cellular distribution of each receptor subtype, is far from being completely understood. Availability of receptor subtype-selective ligands is still critical to our understanding of SRIF's physiological role. Numerous analogues are presently being used in the clinic to manage a number of pathophysiological conditions[4,17–19] and as ligands for radiotherapy.[20,21]

Constraints which reduce the flexibility of peptide-backbones or side-chain orientation have been identified, under certain circumstances, to generate analogues with enhanced biological potency and duration of action or selectivity, stability against proteolytic breakdowns, and improved biodistribution and bioavailability. Such conformational flexibility could allow binding by an induced-fit mechanism, and the analogue could exhibit a conformation accommodating two or more pharmacophores simultaneously.

We have shown that the introduction of DTrp^8 in the octapeptide des-AA^{1,2,4,5,12,13}-SRIF[22,23] resulted in an analogue that binds to all of the five SRIF receptors (sst$_s$) similar to SRIF.[24] DTrp^8 and IAmp^9 substitutions in the undecapeptide des-AA^{1,2,5}-SRIF, DAgl(NMe,2naphthoyl),[8] or L-*threo*-β-Me-Nal[8] in the octapeptide des-AA^{1,2,4,5,12,13}-SRIF resulted in a selective agonist at sst$_1$,[25–29] a selective antagonist at sst$_3$,[30,31] and a selective agonist at sst$_4$,[24,32–34] respectively, by stabilizing the active conformation at these receptors.

The present study describes the synthesis, biological testing, and NMR studies of several analogues of the des-AA^{1,2,4,5,12,13}-[DTrp^8]-SRIF (ODT-8, **1**) scaffold. D-amino acids and/or unnatural amino acids, which reduce or increase the flexibility of the cyclic backbone, aiming to obtain ligands with high binding affinity at the different receptors and sst-selectivity, were used. We have synthesized a series of ODT-8 analogues in which Cys at positions 3 and/or 14 (SRIF numbering) was substituted with DCys, norcysteine (Ncy), D-norcysteine (DNcy),[35] homocysteine (Hcy), and D-homocysteine (DHcy). NMR studies of selected analogues identified structural features that may be responsible for binding to more than one receptor.

Results

Peptide Synthesis and Determination of the Stereochemistry of Ncy in the Peptides. All of the analogues shown in Table 1 were synthesized either manually or automatically on a chloromethylated (CM) resin by using the t-butoxycarbonyl (Boc)-strategy. Boc-Ncy(Mob)-OH, Boc-D/LNcy(Mob)-OH,[35] Boc-Hcy(Mob)-OH, and Boc-DHcy(Mob)-OH were synthesized in our laboratory;[36] see details in the Experimental Section. Peptides containing Ncy at the N-terminus were unstable during hydrogen fluoride cleavage/workup conditions and were acetylated by an excess of acetic anhydride in dichloromethane on the resin before hydrofluoric acid cleavage. All of the Ncy-containing Ac-ODT-8 analogues (**9**–**16**) were synthesized by incorporating racemic Boc-Ncy(Mob)-OH[35] or on racemic Boc-Ncy(Mob)-CM resin. The diastereomeric peptides were separated by reversed-phase high-performance liquid chromatography (RP-HPLC), and the absolute stereochemistry of Ncy in the Ac-ODT-8 analogues was confirmed by the comparison of the HPLC retention times and coelution of each diastereomer with those of the analogues synthesized separately by using

* Corresponding author. Phone: (858) 453-4100. Fax: (858) 552-1546. E-mail: jrivier@salk.edu.

† The Clayton Foundation Laboratories for Peptide Biology, The Salk Institute for Biological Studies.

‡ Structural Biology Laboratory, The Salk Institute for Biological Studies.

§ Institute of Pathology, University of Berne.

[a] Abbreviations: The abbreviations for the common amino acids are in accordance with the recommendations of the IUPAC-IUB Joint Commission on Biochemical Nomenclature (*Eur. J. Biochem.* **1984**, *138*, 9−37). The symbols represent the L-isomer except when indicated otherwise. Additional abbreviations: Boc, t-butoxycarbonyl; Bzl, benzyl; Z(2Cl), 2-chlorobenzyloxycarbonyl; CM, chloromethylated; CZE, capillary zone electrophoresis; CYANA, combined assignment and dynamics algorithm for NMR applications; DHcy, D-homocysteine; DMF, dimethylformamide; DMSO, dimethylsulfoxide; DNcy, D-norcysteine; Hcy, homocysteine; HOBt, 1-hydroxybenzotriazole; IAmp, 4-(N-isopropyl)-aminomethylphenylalanine; IBMX, 3-isobutyl-I-methylxanthine; Mob, 4-methoxybenzyl; Ncy; norcysteine; NOE, nuclear Overhauser enhancement; 3D, three-dimensional; OBzl, benzyl ester; PROSA, Processing algorithms; rmsd, root-mean-square deviation; RP-HPLC, reversed-phase high-performance liquid chromatography; SAR, structure−activity relationship; SRIF, somatostatin; sst$_s$, SRIF receptors; TEA, triethylamine; TEAP, triethylammonium phosphate.

10.1021/jm701444y CCC: $40.75 © 2008 American Chemical Society
Published on Web 04/12/2008

Table 1. Physico-chemical Properties and sst_{1-5} Binding Affinities (IC_{50}, nM) of the Analogues and Control Peptide ODT-8 (**1**)

		purity		MS[c]		IC_{50} (nM)[d]					
ID	compd	HPLC[a]	CZE[b]	M_{calc}	$M + H_{obs}$	sst_1	sst_2	sst_3	sst_4	sst_5	no. of atoms in the cycle
	SRIF-28	99	99	3145.45	3146.46	3.2 ± 0.3 (16)	2.6 ± 0.3 (18)	3.8 ± 0.6 (16)	3.4 ± 0.3 (16)	3.2 ± 0.5 (16)	38
1[e]	ODT-8 [H-c(Cys[3]-Phe[6]-Phe[7]-DTrp[8]-Lys[9]-Thr[10]-Phe[11]-Cys[14])-OH](SRIF numbering)	95	98	1078.45	1078.90	27 ± 3.4 (4)	41 ± 8.7 (6)	13 ± 3.2 (4)	1.8 ± 0.7 (4)	46 ± 27 (3)	26
2	[DCys[3]]-ODT-8	99	99	1078.44	1079.48	14 (11; 17)	14.5 (15; 14)	4.5 (4.4; 4.6)	1.0 (1.2; 0.8)	9.5 (11; 7.9)	26
3[e]	[DCys[14]]-ODT-8	99	99	1078.44	1079.23	>1K (2)	18 (17; 19)	18.5 (20; 17)	8.2 (9; 7.3)	27 (29; 24)	26
4	[DCys[3], DCys[14]]-ODT-8	99	99	1078.44	1079.36	>1K (2)	11 (9; 12)	6.3 (6; 6.6)	2.6 (2.8; 2.4)	8.7 (8.6; 8.8)	26
5	Ac-ODT-8	99	99	1120.45	1121.29	22 ± 8.8 (3)	49 ± 9 (4)	7.1 ± 0.9 (3)	1.3 ± 0.2 (4)	26 ± 12 (3)	26
6	[DCys[3]]Ac-ODT-8	99	97	1120.45	1121.23	16 (19; 13)	8.0 (6.4; 8.6)	19 (7.8; 30)	0.7 ± 0.1 (3)	9.1 (8.9; 9.3)	26
7	[DCys[14]]Ac-ODT-8	99	99	1120.45	1121.26	>1000 (4)	4.9 (5.3; 4.4)	12 (5.5; 18)	4.5 (4.7; 4.3)	11 (12; 10)	26
8	[DCys[3], DCys[14]]Ac-ODT-8	99	99	1120.45	1121.43	>1000 (4)	9 (11; 7)	15 (11; 18)	3.25 (3.3; 3.2)	7.4 (6.2; 8.5)	26
9	[Ncy[3]]Ac-ODT-8	97	98	1106.44	1107.20	79 (107; 50)	33 (39; 26)	6.0 (3.9; 8)	1.9 ± 0.6 (3)	9.0 (5.9; 12)	25
10	[DNcy[3]]Ac-ODT-8	99	97	1106.44	1107.23	416 ± 126 (4)	42 ± 11 (5)	14 ± 2.6 (4)	3.1 ± 0.9 (5)	46 ± 16 (4)	25
11	[Ncy[14]]Ac-ODT-8	99	98	1106.44	1107.18	358 (540; 175)	41 (36; 45)	20 (13; 26)	2.0 ± 0.5 (3)	50 (39; 61)	25
12	[DNcy[14]]Ac-ODT-8	98	99	1106.44	1107.18	>1000 (4)	5.4 (3.6; 7.1)	53 (22; 83)	6.0 (8.1; 3.9)	82 (38; 126)	25
13	[DCys[3], Ncy[14]]Ac-ODT-8	97	96	1106.44	1107.48	540 ± 171 (3)	18.5 (18; 19)	30 (31; 29)	1.5 ± 0.5 (3)	51 (84; 18)	25
14	[DCys[3], DNcy[14]]Ac-ODT-8	99	99	1106.44	1107.48	>1000 (4)	4.8 (4.3; 5.3)	36 (45; 27)	3 ± 0.8 (3)	17 (25; 9.8)	25
15	[Ncy[3], DCys[14]]Ac-ODT-8	99	99	1106.44	1107.44	>1000 (4)	11 (9; 13)	69 (21; 117)	4.4 (5.1; 3.6)	50 (15; 85)	25
16	[DNcy[3], DCys[14]]Ac-ODT-8	97	97	1106.44	1107.45	>1000 (5)	13 ± 2.7 (5)	28 ± 6.1 (4)	5.0 ± 0.6 (4)	50 ± 7.9 (3)	25
17	[Ncy[3], DNcy[14]]Ac-ODT-8	97	98	1092.42	1093.39	>1000 (4)	3.9 (6.2; 1.3)	50 (84; 16)	2.6 ± 0.7 (3)	60 (93; 26)	24
18[e]	[DNcy[3], Ncy[14]]Ac-ODT-8	96	99	1092.42	1093.58	>1000 (2)	109 ± 8.5 (3)	45 (32; 58)	2.7 ± 0.3 (3)	107(163; 51)	24
19[e]	[Ncy[3], Ncy[14]]Ac-ODT-8	99	99	1092.42	1093.37	302 (381; 222)	34 (32; 36)	19 (16; 22)	1.6 ± 0.2 (3)	57 (73; 40)	24
20	[DNcy[3], DNcy[14]]Ac-ODT-8	94	99	1092.42	1093.53	>1000 (4)	13 ± 2.5 (3)	31 (23; 38)	2.2 ± 0.6 (3)	21 (29; 12)	24
21[e]	[Hcy[3]]-Ac-ODT-8	97	98	1134.47	1135.88	96 (103; 89)	6.5 (6.1; 6.9)	38 (59; 17)	0.9 (0.61; 1.1)	28 (17; 38)	27
22	[DHcy[3]]-Ac-ODT-8	98	99	1134.47	1135.64	218 (306; 130)	40 (48; 32)	69 (74; 63)	1.4 (1.3; 1.5)	90 (57; 122)	27

[a] Percent purity determined by HPLC by using buffer system: A = TEAP (pH 2.5) and B = 60% CH_3CN/40% A with a gradient slope of 1% B/min, at a flow rate of 0.2 mL/min on a Vydac C_{18} column (0.21 × 15 cm, 5-μm particle size, 300 Å pore size). Detection at 214 nM. [b] Capillary zone electrophoresis (CZE) was done by using a Beckman P/ACE System 2050 controlled by an IBM Personal System/2 Model 50Z and by using a ChromJet integrator. Field strength of 15 kV at 30 °C, mobile phase: 100 mM sodium phosphate (85:15, H_2O:CH_3CN) pH 2.50, on a Supelco P175 capillary (363 μm o.d. × 75 μm i.d. × 50 cm length). Detection at 214 nM. [c] Calculated *m*/*z* of the monoisotope compared with the observed $[M + H]^+$ monoisotopic mass. [d] The IC_{50} values (nM) were derived from competitive radioligand displacement assays reflecting the affinities of the analogues for the cloned SRIF receptors by using the nonselective ^{125}I-[Leu[8],DTrp[22],Tyr[25]]SRIF-28 as the radioligand. Mean value ± SEM when $N \geq 3$ (shown in parentheses). In the other cases, mean is shown with single values in parentheses. [e] 3D NMR structures of these analogues are presented in this paper.

resolved Boc-Ncy(Mob)-OH. This approach of determining stereochemistry was successful in analogues containing Ncy residue at position 3 (**9**, **10**, **15**, and **16**) but not in analogues containing Ncy at the C-terminus (**11**, **12**, **13**, and **14**). Our attempts to link the Boc-Ncy(Mob)-OH in optically active form to the CM resin failed because racemization occurred during the attachment step (2.0 equiv of KF per mmol of amino acid in dimethylformamide (DMF) at 80 °C for 15 h). It is noteworthy to mention here that optical integrity of the resolved Boc-Ncy(Mob)-OH[35] in peptides **9** and **15** was significantly reduced when coupling was mediated under basic conditions (TBTU/diisopropylethylamine/1-hydroxybenzotriazole (HOBt) in DMF) instead of neutral conditions (*N*,*N*′-diisopropylcarbodiimide/HOBt in DMF). Hence, to determine the stereochemistry of Ac-ODT-8 analogues containing Ncy (**11**–**14**) at the C-terminus, we used an alternative method[28] described by our group for the synthesis of N^{α}-methylated SRIF analogues. On the basis of the premise that failure to attach Boc-Ncy(Mob)-OH in optically active form to the CM resin was due to susceptibility of Ncy residue to racemization under standard coupling conditions, we first synthesized lysine-elongated peptides, that is, [Ncy[14]]Ac-ODT-8-Lys and [DCys[3], Ncy[14]]Ac-ODT-8-Lys, starting with Boc-Lys(2-Cl-Z)-CM resin. The enzymatic hydrolysis of the purified peptides [Ncy[14]]Ac-ODT-8-Lys and [DCys[3], Ncy[14]]Ac-ODT-8-Lys with a carboxypeptidase B enzyme preparation[37] resulted in the desired nonlysine-containing **11** and **13**, respectively. RP-HPLC studies revealed that **9**, **11**, **13**, and **15** synthesized with the resolved Boc-Ncy(Mob)-OH coeluted with the first eluting diastereomer of the pairs **9** + **10**, **11** + **12**, **13** + **14**, and **15** + **16**, respectively. Analogues **17**–**20** were synthesized by using racemic Boc-Ncy(Mob)-OH on racemic Boc-Ncy(Mob)-CM resin. The four diastereomers (**17**–**20**) with retention times of 11.1, 12.3, 13.1, and 14.1 min were separated and purified by RP-HPLC. The stereochemistry of the diastereomers **17, 18**, and **19** was confirmed by comparison of the HPLC retention times and coelution of each diastereomer with those of the analogues obtained from the enzymatic hydrolysis of lysine-extended peptides [Ncy[3], DNcy[14]]Ac-ODT-8-Lys, [DNcy[3], Ncy[14]]Ac-ODT-8-Lys, and [Ncy[3], Ncy[14]]Ac-ODT-8-Lys, respectively. This confirmed that analogue **20** eluting (t_R) at 14.1 min on analytical HPLC contained DNcy at positions 3 and 14.

Purification and Characterization of the Analogues (see Table 1). Purification was carried out by using multiple HPLC steps.[38] Characterization and purity of the analogues were established by HPLC,[38] capillary zone electrophoresis,[39] and mass spectrometry. The C-terminus-extended purified target peptides (RP-HPLC and CZE purity >96%) could be hydrolyzed with carboxypeptidase B, resulting in the desired analogues. The measured masses obtained by matrix-assisted laser desorption ionization mass spectrometry were within 100 ppm of those calculated for the protonated molecule ions and are given in Table 1.

Receptor Binding. The compounds were tested for their ability to bind to the five human sst receptor subtypes (sst_s) in competitive experiments by using ^{125}I-[Leu[8],DTrp[22],Tyr[25]]SRIF-28 as radioligand. Cells stably expressing the five cloned human sst_s were grown as described previously.[3] Cell membrane pellets were prepared, and receptor autoradiography was performed as previously depicted in detail.[3] The binding affinities are expressed as IC_{50} values that are calculated after quantification of the data by using a computer-assisted image processing system as described previously[3,40] and are summarized in Table 1.

Table 2. Characterization of the NMR Structures of the Analogues Studied by NMR[a]

ID	NOE distance restraints	angle restraints[b]	CYANA target function[c]	backbone rmsd (Å)	overall rmsd (Å)	CFF91 energies (kcal/mol) total energy	van der Waals	electro-static	residual restraint violations on distances no ≥ 0.1 Å	distances max (Å)	dihedral angles no ≥ 1.5°	dihedral angles max (°)
1	116	22	0.001	0.65 ± 0.12	1.39 ± 0.21	192.7 ± 18	100.5 ± 3	30.2 ± 2	0.1 ± 0.1	0.04 ± 0.03	0 ± 0	0 ± 0
3	163	18	0.08	0.18 ± 0.09	0.62 ± 0.12	214.3 ± 4	142.7 ± 2	71.6 ± 3	0.9 ± 0.1	0.12 ± 0.04	0 ± 0	0 ± 0
18	110	16	0.08	0.13 ± 0.04	0.72 ± 0.15	178.2 ± 2	132.5 ± 2	45.7 ± 1	0.8 ± 0.0	0.09 ± 0.00	0.9 ± 0	0.9 ± 0.04
19	88	24	0.11	0.72 ± 0.20	1.12 ± 0.15	185.5 ± 6	137.2 ± 6	48.3 ± 8	1.0 ± 0.2	0.15 ± 0.06	0.5 ± 0.5	0.4 ± 0.4
21	111	29	0.015	0.17 ± 0.07	0.79 ± 0.21	193.2 ± 4	143.8 ± 2	49.5 ± 2	0.3 ± 0.1	0.50 ± 0.07	0 ± 0	0 ± 0.04

[a] The bundle of 20 conformers with the lowest residual target function was used to represent the NMR structures of each analogue. [b] Meaningful NOE distance restraints may include intraresidual and sequential NOEs.[42] [c] The target function is zero only if all the experimental distance and torsion angle constraints are fulfilled and all nonbonded atom pairs satisfy a check for the absence of steric overlap. The target function is proportional to the sum of the square of the difference between calculated distance and isolated constraint or van der Waals restraints, and similarly isolated angular restraints are included in the target function. For the exact definition see ref 42.

Analogue **1** binds to the five receptors of SRIF with low nanomolar affinity and has maximum affinity for sst_4. Analogue **2** differs from **1** by a DCys at position 3 and binds to all of the SRIF receptors with higher affinity than analogue **1**. Analogue **3** differs from **1** by a DCys at position 14 and does not bind to sst_1. Acetylation of ODT-8 (**1**) results in **5** that binds to all of the sst_s similar to ODT-8 (**1**). The acetylation of **2** and **3** resulting in **6** and **7** has some influence on the binding affinity of these peptides at sst_2 but not at the other sst_s compared with the parent peptides. Analogue **8** differs from **6** by having a DCys at position 14, and this peptide does not bind to sst_1 but binds to all of the other receptors with a binding affinity similar to that of **6**. Ncy and DNcy substitutions at position 3 for Cys in Ac-ODT-8 (**5**) result in **9** and **10** that bind to all sst_s but sst_1 similar to **5**. Analogues **11** and **13** differ from **5** and **6** by having Ncy at position 14. Both peptides bind to sst_1 with significantly less affinity than the parent analogues. DCys substitution at position 14 has resulted in **15**−**17** showing enhancement in binding affinity for sst_2 compared to **5**. Similarly, DNcy substitution at position 14 resulted in **12**, **14**, **17**, and **20**, which bind to sst_2 with higher affinity than **5**. Analogue **18** differs from **1** by having DNcy at position 3 and Ncy at position 14 and has an acetylated N-terminus. It binds to sst_4 in low nanomolar affinity (IC_{50} = 2.7 nM) and with moderate affinity to receptors sst_2, sst_3, and sst_5 (IC_{50} = 110, 45, and 107 nM, respectively) but does not bind to sst_1. Analogue **19** is similar to **18** except for Ncy residues at position 3. Analogue **19** binds to sst_4 with high affinity (IC_{50} = 1.6 nM) and shows moderate affinity for receptors sst_2, sst_3, and sst_5, (IC_{50} = 34, 19, and 57 nM, respectively) and weak binding affinity to sst_1 (IC_{50} = 302 nM). Analogue **21** differs from **1** by having Hcy at position 3 and has an acetylated N-terminus. It shows high binding affinity for sst_2 and sst_4 (IC_{50} ≈ 6 and 0.8 nM, respectively) but only moderate affinity for the other three receptors. The substitution of Hcy by DHcy in analogue **21** results in analogue **22** that shows lower binding affinity for all of the sst_s than **21**.

To get insights into the action of such nonselective analogues, structural studies were carried out in dimethylsulfoxide (DMSO). The conformation preferred in DMSO may be difficult to interpret because of the nonselective binding of the analogues.

Analogues studied here bind nonselectively to more than one receptor, and hence, it is interesting to compare their 3D structures in DMSO with the available receptor-selective pharmacophores.[29,34,41] Analogues **1**, **3**, **18**, **19**, and **21** (Table 1) have been selected for these studies. They have similar structures except for the stereochemistry of the bridgeheads and the number of atoms involved in the cycle.

NMR Studies. We present details about the chemical shift assignment of proton resonances and structural information for **1**, **3**, **18**, **19**, and **21** (Table 1) obtained by solution-state NMR studies in the solvent DMSO.

Assignment of Proton Resonances, Collection of Structural Restraints, and Structure Determination. Almost all chemical shift assignments of proton resonances (Table S2) for all of the analogues (Table 1, assignment and structural characterization of analogue **1** (ODT-8) have been taken from Grace et al.[34]) have been carried out by using 2D NMR experiments by applying the standard procedure described in the Experimental Section. The N-terminal amino protons for **1** and **3** have not been observed because of fast exchange with the solvent. The N-acetyl terminal amide protons, however, are observed for **18**, **19**, and **21**.

A large number of experimental nuclear Overhauser enhancements (NOEs) have been observed for all of the five analogues in the NOESY spectrum measured with a mixing time of 100 ms, leading to over 100 meaningful distance restraints per analogue and concomitantly ∼10 restraints per residue (Table 2). These structural restraints were used as input for the structure calculation with the program combined assignment and dynamics algorithm for NMR applications (CYANA)[42] followed by restrained energy minimization by using the program DISCOVER.[43] The resulting bundle of 20 conformers per analogue represents the 3D structure of each analogue in DMSO. For each analogue, the small residual constraint violations in the distances for the 20 refined conformers (Table 2) and the coincidence of the experimental NOEs and short interatomic distances (data not shown) indicate that the input data represent a self-consistent set, and that the restraints are well satisfied in the calculated conformers (Table 2). The deviations from ideal geometry are minimal, and similar energy values have been obtained for all of the 20 conformers for each analogue. The quality of the structures determined is furthermore reflected by the small backbone root-mean-square deviation (rmsd) values relative to the mean coordinates of ∼0.5 Å (see Table 2 and Figure 2).

3D Structure of H-c[Cys^3-Phe^6-Phe^7-DTrp^8-Lys^9-Thr^{10}-Phe^{11}-Cys^{14}]-OH (ODT-8) (1). As we published earlier for analogue **1**[34] (Table 1), the backbone torsion angles indicate that a β-turn of type-VIII′ conformation is present around Phe^7-DTrp^8. A turn-like structure is also supported by the medium range $d_{NN}(i, i + 2)$ distance restraints (Figure 1). Although the unshifted resonance for the amide proton of Lys^9 (293−318 K) is indicative of an expected hydrogen bond Lys^{9}NH−O′Phe^6, the carbonyl C═O of Phe^6 is not in a favorable orientation to be involved in a hydrogen bond. The side chain of Phe^6 is in the gauche$^+$ rotamer, Phe^7 is in the trans rotamer, DTrp^8 is in the gauche$^-$ rotamer, and Lys^9 is in the gauche$^+$ rotamer (Table S1). Conclusively, the side chains of DTrp^8 and Phe^7 are

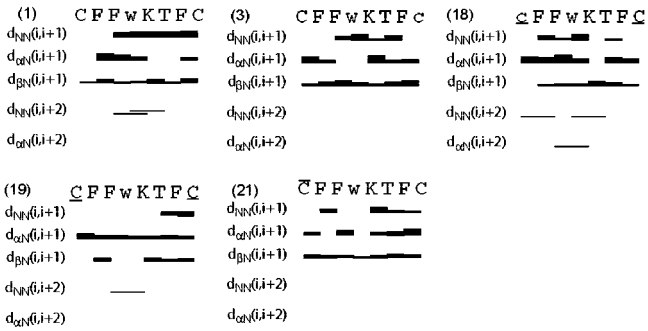

Figure 1. Survey of characteristic NOEs describing the secondary structure of the five analogues studied by NMR (i.e., analogues **1**, **3**, **18**, **19**, and **21** as indicated). Thin, medium, and thick bars represent weak (4.5−6 Å), medium (3−4.5 Å), and strong (<3 Å) NOEs observed in the NOESY spectrum. The medium-range connectivities $d_{NN}(i, i + 2)$, $d_{\alpha N}(i, i + 2)$, and $d_{\beta N}(i, i + 2)$ are shown by lines starting and ending at the positions of the residues related by the NOE. Residues Ncy, DNcy, Hcy, DHcy, DCys, and DTrp refer to norcysteine, D-norcysteine, homocysteine, D-homocysteine, D-cysteine, and D-tryptophan denoted by the symbols, C, c, C̄, c̄, c, and w, respectively.

adjacent to each other in the plane of the analogue backbone, whereas the side chains of Phe^6 and Phe^{11} are pointing away from the plane of the peptide backbone.[34]

3D Structure of H-c[Cys^3-Phe^6-Phe^7-DTrp^8-Lys^9-Thr^{10}-Phe^{11}-DCys^{14}]-OH (3). For analogue **3** (Table 1), the backbone torsion angles do not fit into any of the classified reported β-turns in literature. The side chains of Phe^6, Phe^7, DTrp^8, Lys^9, and Phe^{11} are in the gauche$^+$ rotamer (Table S1). This configuration orients Phe^7, Phe^{11}, and Lys^9 pointing away from the backbone on one side, whereas the side chains of Phe^6 and DTrp^8 point on the opposite side (Figure 2). Ring current of Phe^{11} resulted in slightly upfield-shifted resonances for the γ-protons of Lys^9 (Table S2).

3D Structure of Ac-c[DNcy^3-Phe^6-Phe^7-DTrp^8-Lys^9-Thr^{10}-Phe^{11}-Ncy^{14}]-OH (18). For analogue **18** (Table 1), the backbone torsion angles indicate a β-turn of type-II conformation around Phe^7-DTrp^8 (Table S1). The side chains of Phe^6, DTrp^8, and Lys^9 are in the gauche$^+$ rotamer, Phe^7 is in the trans rotamer, and Phe^{11} is in the gauche$^-$ rotamer (Table S1). Hence, the side chains of Phe^7 and DTrp^8 adjacent to each other are in the plane of the peptide backbone, whereas the side chains of Lys^9 and Phe^6 are in close proximity. The side chain of Phe^{11} is far away from the DTrp^8-Lys^9 pair behind the peptide backbone (Figure 2). Ring current of Phe^6 has resulted in slightly upfield-shifted resonance for the γ-protons of Lys^9. Hydrogen bonds are observed in all of the calculated 20 conformers between the amide protons of Lys^9, Thr^{10}, and the carbonyl of Phe^6 and also between the amide proton of Phe^6 and the carbonyl of Thr^{10}. Experimentally measured small temperature coefficients of −0.02, −0.004, and −0.01 ppm/K for the amide protons of Phe^6, Lys^9, and Thr^{10}, respectively, confirm that these amide protons are involved in the hydrogen bond.

3D Structure of Ac-c[Ncy^3-Phe^6-Phe^7-DTrp^8-Lys^9-Thr^{10}-Phe^{11}-Ncy^{14}]-OH (19). For analogue **19** (Table 1), the backbone torsion angles do not fit into any of the classified β-turns reported in the literature. The side chains of Phe^6, Phe^7, DTrp^8, Lys^9, and Phe^{11} are in the gauche$^+$ rotamer (Table S1). This orients the side chains of Phe^6, Lys^9, and Phe^{11} on one side of the peptide backbone, with Phe^{11} in close proximity to Lys^9. Side chains of Phe^7 and DTrp^8 are in the plane of the peptide backbone (Figure 2).

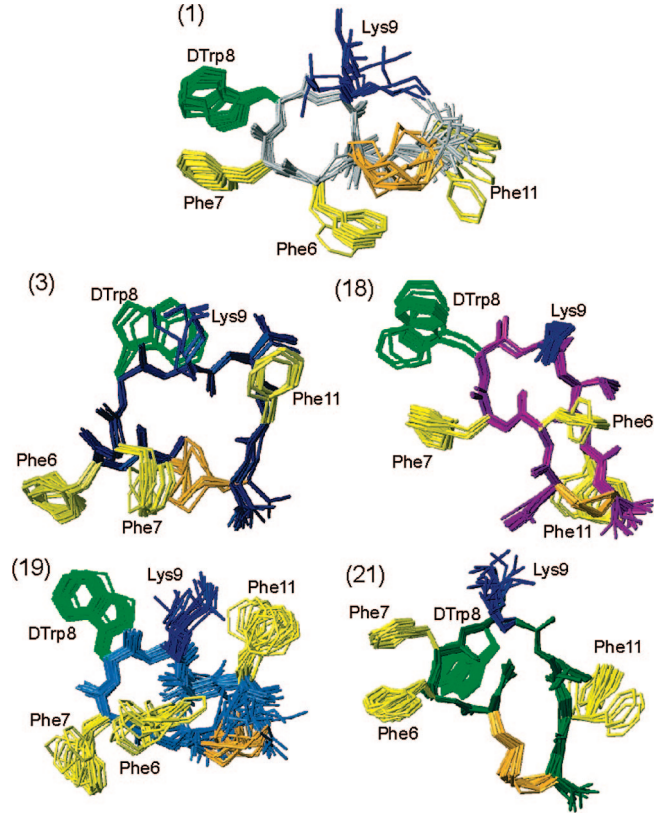

Figure 2. 3D structures of the five analogues studied by NMR (i.e., analogues **1, 3, 18, 19**, and **21** as indicated). For each analogue, 20 energy-minimized conformers with the lowest target function are used to represent the 3D NMR structure. The bundle is obtained by overlapping the C$^\alpha$ atoms of all the residues. The backbone and the side chains are displayed including the disulfide bridge. The following color code is used: gray, (**1**) H-c[Cys-Phe-Phe-DTrp-Lys-Thr-Phe-Cys]-OH, ODT-8 taken from Grace et al.;[34] navy-blue, (**3**) H-c[Cys-Phe-Phe-DTrp-Lys-Thr-Phe-DCys]-OH; violet, (**18**) Ac-c[DNcy-Phe-Phe-DTrp-Lys-Thr-Phe-Ncy]-OH; royal blue, (**19**) Ac-c[Ncy-Phe-Phe-DTrp-Lys-Thr-Phe-Ncy]-OH; and dark green, (**21**) Ac-c[Hcy-Phe-Phe-DTrp-Lys-Thr-Phe-Cys]-OH. The amino acid side chains which are proposed to be involved in binding to the various SRIF receptors are highlighted: light green, DTrp at position 8; blue, Lys at position 9; and yellow, Phe at positions 6, 7, and 11. The disulfide bridges are shown in orange for clarity.

3D Structure of Ac-c[Hcy^3-Phe^6-Phe^7-DTrp^8-Lys^9-Thr^{10}-Phe^{11}-Cys^{14}]-OH (21). The backbone torsion angles from the 3D structures show that an inverse γ-turn is present around DTrp^8 for analogue **21** (Table 1). The side chains of Phe^6, Phe^7, Lys^9, and Phe^{11} are in gauche$^+$ rotamer, and that of DTrp^8 is in gauche$^-$ rotamer (Table S1). This orients the side chains of Phe^6, Phe^7, and Lys^9 on one side of the peptide backbone, whereas the side chains of DTrp^8 and Phe^{11} are on the other side (Figure 2). Close proximity between the amide group of Lys^9 and the carbonyl of Phe^7, as well as the amide group of Thr^{10} and the carbonyl of the acetyl group at the N-terminus, shows possible hydrogen bonds between these groups. Experimentally measured small temperature coefficients of −0.01 and −0.002 ppm/K for the amide protons of Phe^7 and Thr^{10}, respectively, confirm that these amide protons are involved in a hydrogen bond.

Discussion

All of the five analogues studied here by NMR in DMSO bind nonselectively to more than one receptor, and hence, it is interesting to compare their structures with receptor-selective

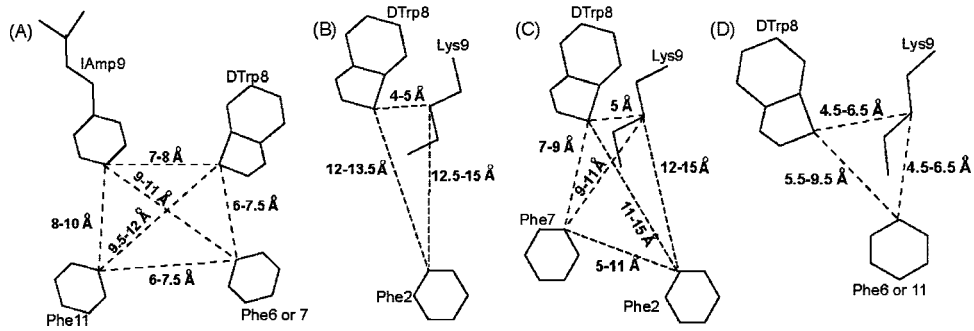

Figure 3. Schematic drawings of agonist pharmacophores for receptor-selective analogues binding to the SRIF receptors. (A) sst_1, (B) sst_2, (C) $sst_{2/5}$, and (D) sst_4. The amino acid side chains, which are part of the pharmacophores, and the distances between the corresponding C_γ atoms of the side chains are shown and are also listed in Table 3.

pharmacophores. However, because of the nonselective binding of these analogues, the elucidation of such a multiple structure-activity relationship (SAR) is not trivial, and a step-by-step analysis is required. Therefore, we first review the structural parameters proposed for the receptor-selective pharmacophores[29,34,41,44] and then discuss the 3D structures of the nonselective analogues of interest.

Pharmacophores of SRIF Receptors. Receptor-selective agonistic analogues binding selectively to SRIF receptors 1, 2, and 4 have been obtained by using both chemical modifications of different amino acid side-chain groups in short SRIF analogues[26,45] and structural design to optimize the pharmacophore.[29,34,41] The pharmacophore for sst_1 binding has been shown to be the $DTrp^8$-$IAmp^9$ (4-(*N*-isopropyl)-aminomethylphenylalanine) pair of residues in addition to two aromatic side chains at positions 7 and 11.[29] On the basis of the pharmacophore and other experimental findings,[25,46] the rationale is that the longer side chain of IAmp can only be accommodated by SRIF receptor 1, whereas, in the other SRIF receptors, the binding cavity is limited to accommodating a smaller side chain as that of Lys. In contrast to the role of the IAmp in receptor selectivity, the two aromatic side chains at positions 7 and 11 are important to enhance the binding to sst_1 (Figure 3A).

Design of an sst_4-selective agonist was more straightforward.[32] The 3D structures of several sst_4-selective analogues identified the pharmacophore for sst_4 to have one aromatic ring of Phe at position 6 or 11 close to Lys^9 in addition to the crucial $DTrp^8$ and Lys^9 pair[34] (Figure 3D). The development of a strictly sst_2-selective analogue appears to be more demanding because analogues binding with nanomolar affinity to SRIF receptor 2 often also bind with high affinity to SRIF receptor 5 and sometimes to receptor 3.[47,48] Most of these partially selective analogues are based on the structure of a SRIF analogue named octreotide and have a type-II′ β-turn in their structure.[44] The octreotide pharmacophore requires two aromatic side chains at positions 7 and 2 in addition to the $DTrp^8$-Lys^9 pair. It has also been shown that octreotide-type analogues undergo conformational change in their backbone from β-sheet to α-helix, resulting in two different positions for the Phe/DPhe/Tyr at position 2.[47] This conformational exchange complicates the basis for receptor selectivity and suggests that two conformations are necessary for an analogue to fit into the two different receptor-selective pharmacophores for receptors 2 and 5 (Figure 3C). Recently, we published data showing that removal of the aromatic side chain at position 7 from an octreotide analogue led to sst_2 selectivity.[41] Hence, the pharmacophore of a sst_2-selective agonist indeed appears to be a subset of the octreotide pharmacophore with one aromatic side chain of Phe^2 in addition to the side chains of the $DTrp^8$-Lys^9 pair. Furthermore, in contrast to octreotide, where Phe^2 undergoes conformational exchange, the sst_2-selective pharmacophore has Phe^2 at a single position (Figure 3B).

Although sst_3-selective agonists have not been reported yet, there is a report on sst_3-selective antagonists, which have aminoglycine at position 8[30] instead of Trp/DTrp, and the structure of this analogue has been reported in water.[31] Similarly, SRIF agonists or antagonists selectively binding to sst_5 have not been described. In summary, selective binding to a receptor requires a unique pharmacophore for the analogues having Trp^8 and Lys^9 (or an amino acid with a different side chain) and a specific number of aromatic residues at the correct distances with respect to each other (Figure 3, Table 3).

Comparison of the 3D Structures of Nonselective SRIF Analogues with Receptor-Selective Pharmacophores. Because shortening or lengthening the side chains of Cys at positions 3 and 14 of Ac-ODT-8 resulted in loss of binding to some receptors, we decided to compare the 3D structures of these nonselective analogues in DMSO to those of the corresponding receptor-selective pharmacophores determined earlier.[29,34,41] All structural data reported above support the fact that the backbone conformation is not responsible for the binding of peptides; it rather acts as a scaffold in orienting the side chains of the analogues to interact efficiently with the receptor. Such conclusions had also been derived on the basis of the NMR structure of astressin (a corticotropin releasing factor antagonist) in DMSO[51] and its bound conformation to the ECD1 of CRF-R2.[49,50]

Hence, the spatial orientations of the amino acid side chains for the different analogues are compared here with those of the receptor-selective pharmacophores. To explain the nonselective binding of an analogue to multiple receptors, either conformational flexibility is necessary to allow binding by an induced-fit mechanism or the analogue prefers a conformation accommodating two or more pharmacophores simultaneously. In particular, the conformation preferred by nonselective analogues in DMSO will not evidently fit all of the pharmacophores simultaneously as proposed.

Comparison of the 3D Structures of the Nonselective Analogues with the sst_1-Selective Pharmacophore. A comparison of the 3D structures of the nonselective analogues with the sst_1-selective pharmacophore shows the following: the introduction of Ncy in the ODT-8 structure (i.e., in **3**, **18**, and **19**) has resulted in loss of binding to receptor 1. Their 3D structures determined in DMSO show that, among the three aromatic residues, two of them are oriented on the front side of the peptide backbone. Because the sst_1 pharmacophore requires two aromatic side chains at the backside of the peptide backbone in addition to Trp^8 and Lys^9 side chains as shown in Figure

Table 3. Distances between C_γ Atoms (in Å) of Selected Residues for the Analogues Studied by NMR and the Selective sst-Pharmacophores

analogue	F^6-F^7	$F^6-{}^DW^8$	F^6-K^9	F^6-F^{11}	$F^7-{}^DW^8$	F^7-K^9	F^7-F^{11}	$^DW^8-K^9$	$^DW^8-F^{11}$	K^9-F^{11}
1	7.2−8.0	10.0−10.2	7.9−9.6	7.6−9.7	4.7−4.9	9.3−10.8	11.8−14.5	7.4−8.9	11.7−13.7	5.9−10.6
3	7.6−7.7	8.4−8.6	11.0−11.7	13.2−13.6	8.0−8.1	5.6−6.5	7.1−8.2	5.7−5.9	8.9−9.4	5.0−5.2
18	8.6−8.6	10.0−10.1	5.4−5.5	8.4−8.9	5.5−5.5	9.4−9.4	8.7−9.9	7.5−7.5	12.0−13.0	11.5−11.6
19	5.1−7.5	7.8−8.6	5.3−7.1	6.6−10.2	7.3−8.2	9.1−10.3	12.6−13.4	5.9−6.2	8.9−10.7	4.4−6.0
21	4.8−5.1	8.7−8.9	7.3−8.0	12.6−13.8	6.4−6.4	5.5−5.7	11.9−13.7	7.0−7.1	6.6−9.5	10.1−10.5
sst_1 pharmacophore					6.0−7.5	9.0−11.0	6.0−7.5	7.0−8.0	9.5−12.0	8.0−10.0
sst_4 pharmacophore	F^2-F^7	5.5−9.5 $F^2-{}^DW^8$	4.5−6.5 F^2-K^9					4.5−6.5	5.5−9.5	4.5−6.5
sst_2 pharmacophore		12.0−13.5	12.5−15.0					4.0−5.0		
octreotide pharmacophore	5.0−11.0	11.0−15.0	12.0−15.0		7.0–9.0	9.0–11.0		5.0−5.0		

3A[29] and Table 3, the sst_1 pharmacophore is not observed in **3, 18**, and **19**. This may explain why **3, 18**, and **19** do not bind to receptor 1. In contrast, the 3D structure of ODT-8 (**1**), which binds to all of the five receptors, has the sst_1 pharmacophore as well.

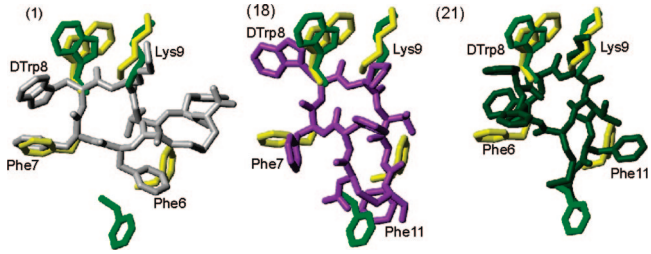

Figure 4. Superposition of receptor-specific pharmacophore with the 3D NMR structure of the analogues **1, 18**, and **21**. The sst_2 pharmacophore[41] is shown in green. The octreotide pharmacophore proposed by Melacini et al.[44] is shown in yellow. In both pharmacophores, only the side chains of the amino acids that are involved in binding to the receptor are shown. For analogues **1, 18**, and **21,** the conformer with the lowest energy is used to represent the 3D structures. The analogues are color-coded as in Figure 2. The side chains of the amino acids, which are proposed to be involved in receptor binding, are labeled. Phe^6 in analogue **1** and Phe^{11} in analogues **18** and **21** should undergo a change in their conformation to fit either the sst_2 or octreotide pharmacophores.

Comparison of the 3D Structures of the Nonselective Analogues with the $Sst_{2,4}$-Selective Pharmacophores. The sst_2-selective pharmacophore requires one aromatic side chain far from the Trp^8-Lys^9 pair in addition to these two side chains, as shown in Figure 3B[41] and Table 3. Although **1**, **3**, **18**, **19**, and **21** bind to receptor 2 with nanomolar affinity, the 3D NMR structures of the analogues in DMSO show that these analogues do not have the sst_2-selective pharmacophore (Figure 4). In **1**, **18**, and **21**, a small conformational change of the side chain of either Phe^6 or Phe^{11} can establish the partially selective pharmacophore (Figure 4). But in **3** and **19**, the side chain of Phe^6 has to undergo a large conformational change to fit the sst_2-selective pharmacophore. Therefore, the 3D structures of the analogues determined in DMSO are not sufficient to explain the $sst_{2,5}$ nonselective pharmacophore.

Also DCys or DNcy substitution at position 14 has resulted in analogues (**3**, **4**, **7**, **8**, **15**, and **16** or **12**, **14**, **17**, and **20**) showing enhanced binding affinity for sst_2 compared to **5**. A D-amino acid, part of the cycle at the C-terminus, changes the backbone conformation, probably bringing the side chains of Phe^{11} close to the sst_2 pharmacophore (Figure 4). In addition, all of these analogues do not bind to sst_1, probably because of the positioning of the side chain of Phe^{11}, critical for sst_1 binding (Figure 3A).

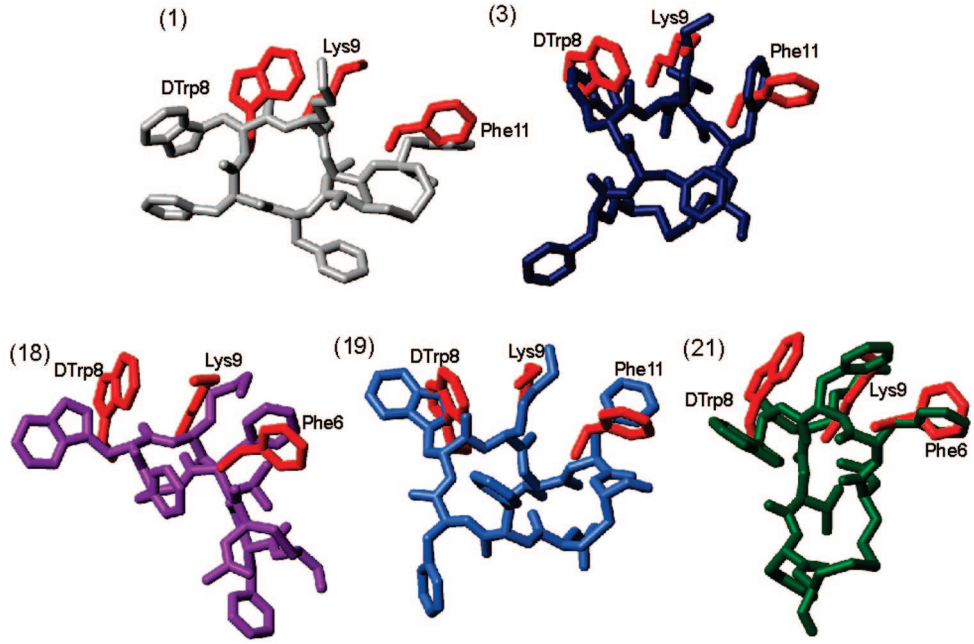

Figure 5. Superposition of sst_4 receptor-specific pharmacophore with the 3D NMR structures of the analogues **1**, **3**, **18**, **19**, and **21**. The sst_4 pharmacophore[34] is represented by amino acid side chains colored in red. The conformer with the lowest energy represents the 3D structures of the analogues, and they are color-coded as in Figure 2. In addition, for each analogue, the amino acid side chains proposed to be involved in receptor binding are labeled.

However, these analogues have the highest affinity for receptor 4, and the sst_4 pharmacophore is present in their conformations. The sst_4-selective pharmacophore requires one aromatic side chain close to Lys^9 in addition to the side chains of Trp^8 and Lys^9, as shown in Figure 3C. The distances between the C_γ atoms of the side chains to fit the sst_4 pharmacophore are given in Table 3. The 3D structures of **1**, **3**, **18**, **19**, and **21** have the sst_4 pharmacophore as shown in Figure 5, with either Phe^{11} (**1**, **3**, and **19**) or Phe^6 (**18** and **21**) involved in sst_4 binding in addition to the necessary $DTrp^8$ and Lys^9 side chains.

Conclusions

Synthesis, binding, and 3D NMR structure of nonselective analogues of H-c(Cys-Phe-Phe-DTrp-Lys-Thr-Phe-Cys)-OH (ODT-8, **1**) containing different side chain lengths for the Cys at positions 3 and 14 have been presented here. These analogues bind nonselectively to all of the five SRIF receptors, and the elucidation of a SAR is challenging. In our attempt to establish such a relationship between the 3D structures of the analogues determined in DMSO and their receptor specificity, it has been observed that the 3D structures mostly have the pharmacophore for which the analogues have the highest binding affinities. All of these analogues bind to sst_4 with the highest binding affinity, and their 3D structures have the sst_4 pharmacophore. However, the pharmacophores of the other receptors are often not covered by the 3D structure determined in DMSO, and their pharmacophores can only be established by reorientation of some of the amino acid side chains.

The establishment of receptor-selective and nonselective analogues of SRIF by introducing small chemical modifications to the peptides highlights the complexity of a binding event. The structure determination of these analogues in DMSO elucidates thereby, at least in part, the nature of this complexity.

Experimental Section

Determination of the Stereochemistry of Ncy^{14} in the Analogues. The fully protected Ac-Ncy(Mob)^3-Phe^6-Phe^7-DTrp^8-Lys(2-Cl-Z)^9-Thr(Bzl)^{10}-Phe^{11}-Ncy(Mob)^{14}-Lys(2-Cl-Z)^{15}-CM resin (SRIF numbering) was synthesized, cleaved from the resin by hydrofluoric acid, cyclized and purified on preparative RP-HPLC. The purified peptide Ac-[Ncy^3-Phe^6-Phe^7-DTrp^8-Lys^9-Thr^{10}-Phe^{11}-Ncy^{14}]-Lys^{15}-OH (20 mg, 16.30 μM) was hydrolyzed in 0.1 M NaCl−0.05 M Tris buffer at pH 7.6 (20 mL) with undiluted carboxypeptidase B enzyme solution (50 U) at room temperature. The hydrolysis was complete in 30 min, resulting in analogue **19** (Table 1). The product was desalted by preparative RP-HPLC, and pure peptide **19** (12 mg, 10.9 μM) was obtained (yield of hydrolysis: 66.87%). Analogues **11**, **13**, **17**, and **18** were obtained from the lysine-extended peptides [Ncy^{14}]Ac-ODT-8-Lys, [DCys^3, Ncy^{14}]Ac-ODT-8-Lys, [Ncy^3, DNcy^{14}]Ac-ODT-8-Lys, and [DNcy^3, Ncy^{14}]Ac-ODT-8-Lys, respectively, in comparable yields by using this protocol.

Cell Culture. CHO-K1 cells stably expressing human sst_1 and sst_5 were kindly provided by Dr. T. Reisine and Dr. G. Singh (University of Pennsylvania, Philadelphia, PA), and CCL39 cells stably expressing human sst_1, sst_2, sst_3, and sst_4 were provided by Dr. D. Hoyer (Novartis Pharma, Basel, Switzerland). Cells were grown as described previously.[3] All culture reagents were supplied by Gibco BRL (Life Technologies, Grand Island, NY).

Receptor Binding. Cell membrane pellets were prepared, and receptor autoradiography was performed as depicted in detail previously.[3] Binding studies were performed as reported previously[3] with [Leu^8,DTrp^{22},^{125}ITyr^{25}]-SRIF-28 on cell pellet sections and on tissue sections of the respective sst-expressing human tumors by using 15 000 cpm/100 μL of the radioligand.

Sample Preparation and NMR Experiments. NMR samples were prepared by dissolving 2 mg of the analogue in 0.5 mL of DMSO-d_6. The ^{1}H NMR spectra were recorded on a Bruker 700 MHz spectrometer operating at a proton frequency of 700 MHz as reported previously.[29,34,41,51]

Structure Determination. The chemical shift assignment of the major conformer (the population of the minor conformer was <10%) was obtained by the standard procedure by using double quantum filtered correlation spectroscopy and total correlation spectroscopy spectra for intraresidual assignment, and the NOESY spectrum was used for the sequential assignment.[52] The collection of structural restraints was based on the NOEs assigned manually and vicinal $^3J_{NH\alpha}$ couplings. Dihedral angle constraints were obtained from the $^3J_{NH\alpha}$ couplings, which were measured from the 1D ^{1}H NMR spectra and from the intraresidual and sequential NOEs, along with the macro GRIDSEARCH in the program CYANA.[42] The calibration of NOE intensities versus ^{1}H−^{1}H distance restraints and appropriate pseudoatom corrections to the nonstereo specifically assigned methylene, methyl, and ring protons were performed by using the program CYANA. On average, approximately 100 NOE constraints and 20 angle constraints were utilized to calculate the conformers (Table 2). A total of 100 conformers were initially generated by CYANA, and a bundle containing 20 CYANA conformers with the lowest target function values were utilized for further restrained energy minimization by using the CFF91 force field[53] with the energy criteria fit 0.1 kCal/mol/Å [54] in the program DISCOVER with steepest decent and conjugate gradient algorithms.[55] The resulting energy-minimized bundle of 20 conformers was used as a basis for discussing the solution conformation of the different SRIF analogues. The structures were analyzed by using the program MOLMOL.[56]

Acknowledgment. This work was supported in part by NIH grant R01 DK059953. We are indebted to R. Kaiser and C. Miller for technical assistance in the characterization of the peptides, Dr. W. Fisher and W. Low for mass spectrometric analysis of the analogues, and D. Doan for manuscript preparation. J.R. is the Dr. Frederik Paulsen Chair in Neurosciences Professor.

Supporting Information Available: Starting materials, peptide synthesis, cleavage and deprotection with HF, and cyclization are reported in Supporting Information along with Table S1 (torsion angles φ, Ψ, and χ_1 (in °) for the bundle of 20 energy-minimized conformers) and Table S2 (proton chemical shifts of the analogues studied by NMR). This material is available free of charge via the Internet at http://pubs.acs.org.

References

(1) Brazeau, P.; Vale, W.; Burgus, R.; Ling, N.; Butcher, M.; Rivier, J.; Guillemin, R. Hypothalamic polypeptide that inhibits the secretion of immunoreactive pituitary growth hormone. *Science* **1973**, *179*, 77–79.

(2) Guillemin, R.; Gerich, J. E. Somatostatin: Physiological and clinical significance. *Annu. Rev. Med.* **1976**, *27*, 379–388.

(3) Reubi, J. C.; Schaer, J. C.; Waser, B.; Wenger, S.; Heppeler, A.; Schmitt, J. S.; Mäcke, H. R. Affinity profiles for human somatostatin receptor sst1-sst5 of somatostatin radiotracers selected for scintigraphic and radiotherapeutic use. *Eur. J. Nucl. Med.* **2000**, *27*, 273–282.

(4) Janecka, A.; Zubrzycka, M.; Janecki, T. Review: Somatostatin analogs. *J. Pept. Res.* **2001**, *58*, 91–107.

(5) Schally, A. V.; Comaru-Schally, A. M.; Nagy, A.; Kovacs, M.; Szepeshazi, K.; Plonowski, A.; Varga, J. L.; Halmos, G. Hypothalamic hormones and cancer. *Front. Neuroendocrinol.* **2001**, *22*, 248–291.

(6) Lamberts, S. W.; van der Lely, A. J.; Hofland, L. J. New somatostatin analogs: Will they fulfill old promises. *Eur. J. Endocrinol.* **2002**, *146*, 701–705.

(7) Weckbecker, G.; Lewis, I.; Albert, R.; Schmid, H. A.; Hoyer, D.; Bruns, C. Opportunities in somatostatin research: Biological, chemical and therapeutic aspects. *Nat. Rev. Drug Discovery* **2003**, *2*, 999–1017.

(8) van der Hoek, J.; Hofland, L. J.; Lamberts, S. W. Novel subtype specific and universal somatostatin analogues: Clinical potential and pitfalls. *Curr. Pharm. Des.* **2005**, *11*, 1573–1592.

(9) Reubi, J. C. Peptide receptors as molecular targets for cancer diagnosis and therapy. *Endocr. Rev.* **2003**, *24*, 389–427.

(10) Panteris, V.; Karamanolis, D. G. The puzzle of somatostatin: Action, receptors, analogues and therapy. *Hepato-Gastroenterology* **2005**, *52*, 1771–1781.
(11) Petersenn, S. Efficacy and limits of somatostatin analogs. *J. Endocrinol. Invest.* **2005**, *28*, 53–57.
(12) Tulipano, G.; Schulz, S. Novel insights in somatostatin receptor physiology. *Eur. J. Endocrinol.* **2007**, *156*, S3–S11.
(13) Reisine, T.; Bell, G. I. Molecular biology of somatostatin receptors. *Endocr. Rev.* **1995**, *16*, 427–442.
(14) Csaba, Z.; Dournaud, P. Cellular biology of somatostatin receptors. *Neuropeptides* **2001**, *35*, 1–23.
(15) Moller, L. N.; Stidsen, C. E.; Hartmann, B.; Holst, J. J. Somatostatin receptors. *Biochim. Biophys. Acta* **2003**, *1616*, 1–84.
(16) Olias, G.; Viollet, C.; Kusserow, H.; Epelbaum, J.; Meyerhof, W. Regulation and function of somatostatin receptors. *J. Neurochem.* **2004**, *89*, 1057–1091.
(17) Reubi, J. C.; Waser, B.; Liu, Q.; Laissue, J. A.; Schonbrunn, A. Subcellular distribution of somatostatin sst2A receptors in human tumors of the nervous and neuroendocrine systems: Membranous versus intracellular location. *J. Clin. Endocrinol. Metab.* **2000**, *85*, 3882–3891.
(18) Lewis, I.; Bauer, W.; Albert, R.; Chandramouli, N.; Pless, J.; Weckbecker, G.; Bruns, C. A novel somatostatin mimic with broad somatotropin release inhibitory factor receptor binding and superior therapeutic potential. *J. Med. Chem.* **2003**, *46*, 2334–2344.
(19) Reubi, J. C.; Waser, B.; Schaer, J.-C.; Laissue, J. A. Somatostatin receptor sst1-sst5 expression in normal and neoplastic human tissues using receptor autoradiography with subtype-selective ligands. *Eur. J. Nucl. Med.* **2001**, *28*, 836–846.
(20) Reubi, J. C.; Macke, H. R.; Krenning, E. P. Candidates for peptide receptor radiotherapy today and in the future. *J. Nucl. Med.* **2005**, *46*, 67S–75S.
(21) Eberle, A. N.; Mild, G.; Froidevaux, S. Receptor-mediated tumor targeting with radiopeptides. Part 1. General concepts and methods: Applications to somatostatin receptor-expressing tumors. *J. Recept. Signal Transduction Res.* **2004**, *24*, 319–455.
(22) Vale, W.; Rivier, C.; Brown, M.; Rivier, J. Pharmacology of TRF, LRF and somatostatin. *Hypothalamic Peptide Hormones and Pituitary Regulation: Advances in Experimental Medicine and Biology*; Plenum Press: New York, 1977; pp 123–156.
(23) Vale, W.; Rivier, J.; Ling, N.; Brown, M. Biologic and immunologic activities and applications of somatostatin analogs. *Metabolism* **1978**, *27*, 1391–1401.
(24) Rivier, J.; Erchegyi, J.; Hoeger, C.; Miller, C.; Low, W.; Wenger, S.; Waser, B.; Schaer, J.-C.; Reubi, J. C. Novel sst_4-selective somatostatin (SRIF) agonists. Part I: Lead identification using a betide scan. *J. Med. Chem.* **2003**, *46*, 5579–5586.
(25) Chen, L.; Hoeger, C.; Rivier, J.; Fitzpatrick, V. D.; Vandlen, R. L.; Tashjian, A. H., Jr. Structural basis for the binding specificity of a SSTR1-selective analog of somatostatin. *Biochem. Biophys. Res. Commun.* **1999**, *258*, 689–694.
(26) Rivier, J. E.; Hoeger, C.; Erchegyi, J.; Gulyas, J.; DeBoard, R.; Craig, A. G.; Koerber, S. C.; Wenger, S.; Waser, B.; Schaer, J.-C.; Reubi, J. C. Potent somatostatin undecapeptide agonists selective for somatostatin receptor 1 (sst1). *J. Med. Chem.* **2001**, *44*, 2238–2246.
(27) Rivier, J. E.; Kirby, D. A.; Erchegyi, J.; Waser, B.; Eltschinger, V.; Cescato, R.; Reubi, J. C. Somatostatin receptor 1 selective analogues: 3. Dicyclic peptides. *J. Med. Chem.* **2005**, *48*, 515–522.
(28) Erchegyi, J.; Hoeger, C. A.; Low, W.; Hoyer, D.; Waser, B.; Eltschinger, V.; Schaer, J.-C.; Cescato, R.; Reubi, J. C.; Rivier, J. E. Somatostatin receptor 1 selective analogues: 2. N-methylated scan. *J. Med. Chem.* **2005**, *48*, 507–514.
(29) Grace, C. R. R.; Durrer, L.; Koerber, S. C.; Erchegyi, J.; Reubi, J. C.; Rivier, J. E.; Riek, R. Somatostatin receptor 1 selective analogues: 4. Three-dimensional consensus structure by NMR. *J. Med. Chem.* **2005**, *48*, 523–533.
(30) Reubi, J. C.; Schaer, J.-C.; Wenger, S.; Hoeger, C.; Erchegyi, J.; Waser, B.; Rivier, J. SST3-selective potent peptidic somatostatin receptor antagonists. *Proc. Natl. Acad. Sci. U.S.A.* **2000**, *97*, 13973–13978.
(31) Gairi, M.; Saiz, P.; Madurga, S.; Roig, X.; Erchegyi, J.; Koerber, S. C.; Reubi, J. C.; Rivier, J. E.; Giralt, E. Conformational analysis of a potent SSTR3-selective somatostatin analogue by NMR in water solution. *J. Pept. Sci.* **2006**, *12*, 82–91.
(32) Erchegyi, J.; Penke, B.; Simon, L.; Michaelson, S.; Wenger, S.; Waser, B.; Cescato, R.; Schaer, J.-C.; Reubi, J. C.; Rivier, J. Novel sst_4-selective somatostatin (SRIF) agonists. Part II: Analogues with β-methyl-3-(2-naphthyl)-alanine substitutions at position 8. *J. Med. Chem.* **2003**, *46*, 5587–5596.
(33) Erchegyi, J.; Waser, B.; Schaer, J.-C.; Cescato, R.; Brazeau, J. F.; Rivier, J.; Reubi, J. C. Novel sst_4-selective somatostatin (SRIF) agonists. Part III: Analogues amenable to radiolabeling. *J. Med. Chem.* **2003**, *46*, 5597–5605.
(34) Grace, C. R. R.; Erchegyi, J.; Koerber, S. C.; Reubi, J. C.; Rivier, J.; Riek, R. Novel sst_4-selective somatostatin (SRIF) agonists. Part IV: Three-dimensional consensus structure by NMR. *J. Med. Chem.* **2003**, *46*, 5606–5618.
(35) Samant, M. P.; Rivier, J. E. Norcystine, a new tool for the study of the structure-activity relationship of peptides. *Org. Lett.* **2006**, *8*, 2361–2364.
(36) Armstrong, M. D.; Lewis, J. D. Thioether derivatives of cysteine and homocysteine. *J. Org. Chem.* **1950**, *16*, 749–753.
(37) Ambler, R. P. *Methods in Enzymology*; Academic Press: New York, 1967; p 437.
(38) Miller, C.; Rivier, J. Peptide chemistry: Development of high-performance liquid chromatography and capillary zone electrophoresis. *Biopolym. Pept. Sci.* **1996**, *40*, 265–317.
(39) Miller, C.; Rivier, J. Analysis of synthetic peptides by capillary zone electrophoresis in organic/aqueous buffers. *J. Pept. Res.* **1998**, *51*, 444–451.
(40) Reubi, J. C.; Schaer, J. C.; Waser, B.; Hoeger, C.; Rivier, J. A selective analog for the somatostatin sst1-receptor subtype expressed by human tumors. *Eur. J. Pharmacol.* **1998**, *345*, 103–110.
(41) Grace, C. R. R.; Erchegyi, J.; Koerber, S. C.; Reubi, J. C.; Rivier, J.; Riek, R. Novel sst_2-selective somatostatin agonists. Three-dimensional consensus structure by NMR. *J. Med. Chem.* **2006**, *49*, 4487–4496.
(42) Güntert, P.; Mumenthaler, C.; Wüthrich, K. Torsion angle dynamics for NMR structure calculation with the new program DYANA. *J. Mol. Biol.* **1997**, *273*, 283–298.
(43) Hagler, A. T.; Dauber, P.; Osguthorpe, D. J.; Hempel, J. C. Dynamics and conformational energetics of a peptide hormone: Vasopressin. *Science* **1985**, *227*, 1309–1315.
(44) Melacini, G.; Zhu, Q.; Osapay, G.; Goodman, M. A refined model for the somatostatin pharmacophore: Conformational analysis of lanthionine-sandostatin analogs. *J. Med. Chem.* **1997**, *40*, 2252–2258.
(45) Erchegyi, J.; Hoeger, C.; Wenger, S.; Waser, B.; Schaer, J.-C.; Reubi, J. C.; Rivier, J. E. N-methyl scan of a sst1-selective somatostatin (SRIF) analog. In *Peptides -The wave of the future: 2nd International Peptide Symposium/17th American Peptide Symposium*; American Peptide Symposium: San Diego, CA, 2001; pp 719–720.
(46) Liapakis, G.; Fitzpatrick, D.; Hoeger, C.; Rivier, J.; Vandlen, R.; Reisine, T. Identification of ligand binding determinants in the somatostatin receptor subtypes mSSTR1 and mSSTR2. *J. Biol. Chem.* **1996**, *271*, 20331–20339.
(47) Melacini, G.; Zhu, Q.; Goodman, M. Multiconformational NMR analysis of sandostatin (octreotide): Equilibrium between β-sheet and partially helical structures. *Biochemistry* **1997**, *36*, 1233–1241.
(48) Osapay, G.; Prokai, L.; Kin, H.-S.; Medzihradszky, K. F.; Coy, D. H.; Liapakis, G.; Reisine, T.; Melacini, G.; Zhu, Q.; Wang, S. H.-H.; Mattern, R.-H.; Goodman, M. Lanthionine-somatostatin analogs: Synthesis, characterization, biological activity, and enzymatic stability studies. *J. Med. Chem.* **1997**, *40*, 2241–2251.
(49) Grace, C. R. R.; Perrin, M.; DiGruccio, M.; Miller, C.; Rivier, J.; Vale, W.; Riek, R. NMR structure and peptide hormone binding site of the first extracellular domain of a type B1 G-protein coupled receptor. *Proc. Natl. Acad. Sci. U.S.A.* **2004**, *101*, 12836–12841.
(50) Grace, C. R. R.; Perrin, M.; Gulyas, J.; DiGruccio, M.; Cantle, J. P.; Rivier, J.; Vale, W.; Riek, R. Structure of the N-terminal domain of a type B1 G-protein coupled receptor in complex with a peptide ligand. *Proc. Natl. Acad. Sci. U.S.A.* **2007**, *104*, 4858–4863.
(51) Grace, C. R. R.; Cervini, L.; Gulyas, J.; Rivier, J.; Riek, R. Astressin-amide and astressin-acid are structurally different in DMSO. *Biopolymers* **2007**, *87*, 196–205.
(52) Wüthrich, K. *NMR of Proteins and Nucleic Acids*; J. Wiley & Sons: New York, 1986.
(53) Maple, J. R.; Thacher, T. S.; Dinur, U.; Hagler, A. T. Biosym force field research results in new techniques for the extraction of inter- and intramolecular forces. *Chem. Des. Auto. News* **1990**, *5*, 5–10.
(54) Koerber, S. C.; Rizo, J.; Struthers, R. S.; Rivier, J. E. Consensus bioactive conformation of cyclic GnRH antagonists defined by NMR and molecular modeling. *J. Med. Chem.* **2000**, *43*, 819–828.
(55) Hagler, A. T. Theoretical simulation of conformation, energetics and dynamics of peptides. *The Peptides: Analysis, Synthesis, Biology*; Academic Press: Orlando, FL, 1985; pp 213–299.
(56) Koradi, R.; Billeter, M. MOLMOL: A program for display and analysis of macromolecular structures. *PDB Newsletter* **1998**, *84*, 5–7.

JM701444Y